Biochemical and Biophysical Research Communications 448 (2014) 418–423

Contents lists available at ScienceDirect

Biochemical and Biophysical Research Communications

journal homepage: www.elsevier.com/locate/ybbrc

Functional artificial luciferases as an optical readout for bioassays

Sung Bae Kim *, Hiroshi Izumi

Research Institute for Environmental Management Technology, National Institute of Advanced Industrial Science and Technology (AIST), 16-1 Onogawa, Tsukuba 305-8569, Japan

ARTICLE INFO

Article history:
Received 18 April 2014
Available online 4 May 2014

Keywords:
Luciferase
Bioluminescence
Copepod
Epitope
Imaging

ABSTRACT

This study elucidates functional artificial luciferases (ALucs) wholly synthesized for bioassays and molecular imaging. The ALucs bearing epitopes were newly created by amending the sequences of our previously reported ALucs in light of a multi-sequence alignment and hydrophobicity search. The synthesized ALucs are survived in live cells and stable in culture media for 25 days after secretion. The epitopes in ALucs are exposed during the secretion process and indeed valid for column purification and immunological assays. The ALucs exerted a 9400-times stronger optical intensity with a coelenterazine derivative (CTZ *i*), when compared with *Renilla reniformis* luciferase 8.6–535. A supersecondary structure of ALuc30 was predicted with respect to the X-ray crystallographic information of the coelenterazine-binding protein (CBP). The structure revealed that ALuc30 has a room for accommodating the iodide of CTZ *i*. This study guides on how to create functional artificial luciferases and predicts the structural details with the current bioinformatics technologies.

1. Introduction

Bioluminescence is an excellent optical readout for bioanalysis and molecular imaging, which is generated by luciferase catalysis of luciferin to oxyluciferin [1]. To date, many luciferase genes have been cloned from luminescent organisms via the great devotion of many researchers with time-consuming protocols from the reverse synthesis of cDNA from mRNA to identification of the sequence in databases [2].

As the luciferase sequences are accumulated in public databases, an alignment of many relative luciferase sequences facilitates new insights on the phylogenetic history, structural information, consensus amino acids, and much more information [3].

A sequence alignment, called "consensus sequence-driven mutagenesis strategy (CSMS)" was conventionally tried to find consensus amino acids and mutagenesis sites [4]. This approach is based on the premise that frequently occurring amino acids at a given position allow a larger thermostabilizing effect than less-frequent amino acids. Another bioinformatics analysis of multiple sequence alignments, called "statistical coupling analysis (SCA)" was successfully introduced to explain the evolutionary constraints of proteins [5].

Recently, we demonstrated an approach to artificially construct whole amino acid sequences of artificial luciferases (named ALuc), whose identities are distinctive from any existing luciferases [6]. The ALucs have been made by an extraction-and-linkage strategy of frequently occurring amino acids from an alignment of many existing copepod luciferases in public databases, where copepod luciferases were selected because they are the smallest ones among luciferases, exert busting bioluminescence, are genetically conserved, and carry two-repeated catalytic domains like a mirror image [7]. As many ALucs are created with distinctive sequential identities, the useful molecular design and functionalities of ALucs is an intriguing subject in this stage. Epitope- or affinity peptide-tagging schemes are powerful for expending the utilities of luciferases in bioassays. However, a conventional tagging scheme is invalid for copepod luciferases, because the N-terminal is naturally dissected and the C-terminal tagging invades the optical intensities.

This study first demonstrates creation of versatile ALucs embedding epitopes in the middle of the N-terminal region for the broad use in bioassays *in vivo* and *in vitro*, instead of conventional terminal-tagging schemes of an epitope. The epitope-embedding ALucs are designed to expose the epitope during the secretion process and to allow a column-affinity purification and immunological recognition besides bioluminescence imaging (BLI) in complex context of living subjects and *in vitro* assays. The long- and short-term optical stability of the luciferases after secretion is discussed. The characteristic substrate selectivity of ALucs was highlighted with respect to the chemical structures of the substrates. Supersecondary structures of the ALucs were predicted according to a template-based modeling (TBM) with the X-ray crystallographic information on a coelenterazine-binding protein (CBP) from *Renilla muelleri*.

* Corresponding author.
E-mail address: kimu-sb@aist.go.jp (S.B. Kim).

http://dx.doi.org/10.1016/j.bbrc.2014.04.128
0006-291X/

The structural characteristics were briefly discussed with respect to the substrate selectivity and the knowledge on the structures of photoproteins.

2. Methods

2.1. Synthesis of artificial luciferases

The cDNA constructs encoding ALucs 26–34 were custom-synthesized by Operon (Tokyo, Japan) in light of the sequences of ALuc23 and ALuc25, listed in Suppl. Fig. 1. Particularly, the sequences encoding ALucs 26–29 were created by replacing the codons encoding amino acids E^{150}, K^{179}, A^{182}, D^{197}, A^{209} in ALuc25 with codons encoding the corresponding amino acids of Suppl. Fig. 1, while the sequences of ALucs 30–34 were made by substituting the codons encoding amino acids from P20 to V30 in the N-terminal region of ALuc23 with codons encoding the epitope sequences of His×8 (HHHHHHHH, ALuc30 or ALuc31), *c*-Myc (EQKLISEEDL, ALuc32), hemagglutinin (HA) (YPYDVPDYA, ALuc33), or Flag tags (DYKDDDDK, ALuc34). The reason that we chose the region from P^{20} to V^{30} in the sequence is that the amino acids in the region share high sequential homogeneity with the epitopes according to a multiple alignment with CLUSTALW ver2.1 (NCBI). Because the made ALucs are supposed to be secreted by a secretion peptide (SP) at the N-terminal end, an endoplasmic reticulum (ER) retention signal (i.e., KDEL) was further tagged at the C-terminal end for repressing the secretion nature. The made cDNA constructs were subcloned into pcDNA 3.1(+) (Invitrogen) and the fidelity was ensured with a genetic sequence analyzer GenomeLab GeXP (Beckman Coulter). The schematic utilities of the made ALucs was briefly illustrated in Fig. 1A and B. As the internal references, the pcDNA 3.1(+) plasmids encoding *Gaussia princeps* luciferase (GLuc), a variant of *Renilla reniformis* luciferase (RLuc8.6–535), and *Metridia pacifica* luciferase 1 (MpLuc1) were obtained from our previous study [8]. They carry the same ER retention signal (KDEL) at the C-terminal end as ALucs for the fair comparison.

2.2. Identification of the synthesized ALucs

The phylogenetic correlation and maximal sequential identities of the made ALuc sequences when compared with the existing luciferases were determined using public tools provided by NCBI (Protein Blast and CLUSTALW ver2.1). The consequent phylogenetic tree with branch length was specified in Fig. 1C and the aligned sequence and the maximal similarity ranking are shown in Suppl. Fig. 1. The sequence of ALuc30 was aligned in three with CLUSTALW ver2.1 to investigate the internal sequential similarity (named single-sequence alignment (SSA); Fig. 1D). The stop codon at the 3′ end of cDNA encoding ALuc30 is sandwiched between *BamH*I and *Xho*I sites, and followed by cDNA encoding a membrane localization signal (MLS). This characteristic terminal design was previously reported by us and named "a bioluminescent capsule," which can carry any cargo proteins into the PM [9]. Owing to this terminal design, any cDNA encoding a protein of interest is easily inserted between *BamH*I and *Xho*I sites.

2.3. Relative optical intensities and stabilities of ALucs

The relative optical intensities and long-term stabilities of ALucs were determined for evaluating the utilities as an optical readout (Fig. 2A).

African green monkey kidney-derived COS-7 cells raised in a 96-well microplate (Nunc) were transiently transfected with an aliquot (0.1 μg per well) of a plasmid encoding one of ALucs

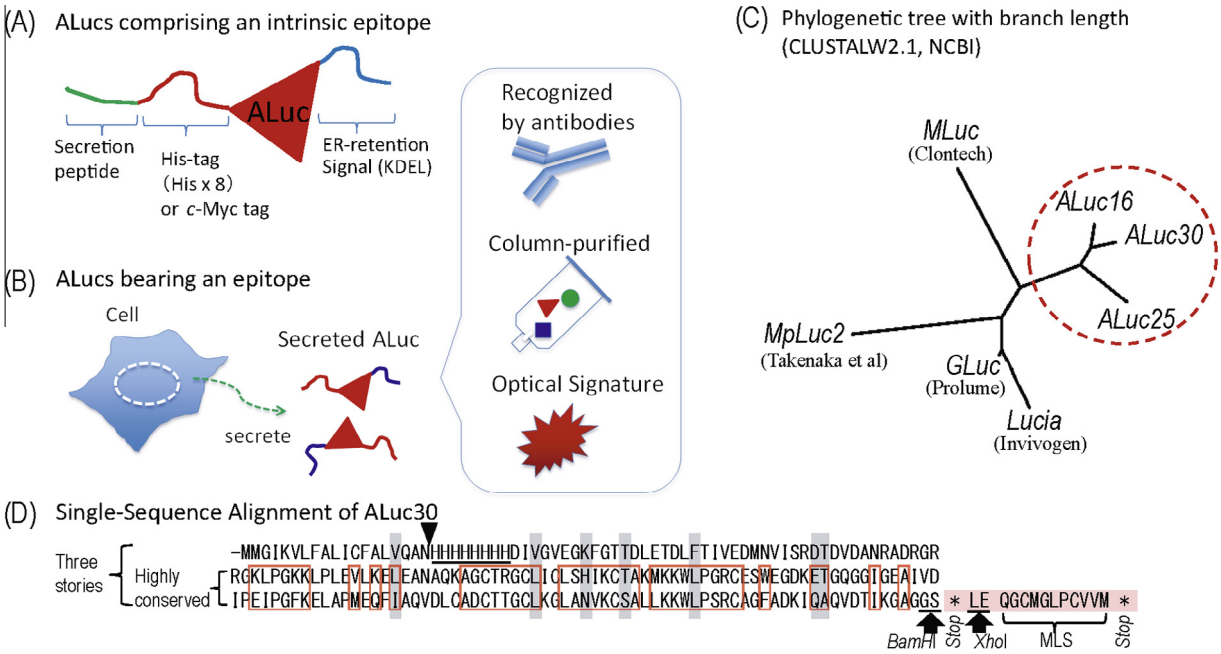

Fig. 1. Establishment of new functional artificial luciferases and the phylogenetic location in light of existing copepod luciferases. (A) Schematic diagram of ALucs 30–34. The epitopes are located in the downstream of the secretion peptide. (B) Brief illustration of the functional ALuc secreted from the host cells for immunoassay, affinity column purification, and bioluminescence assay. ALucs are naturally secreted to the extracellular compartment for column purification or immunoassays. (C) Phylogenetic tree of the existing commercial copepod luciferases and ALucs. The branch lengths reflect the relative phylogenetic distance from each other. The dotted circle indicates the relative phylogenetic location of ALucs in the tree. *Metridia pecifica* luciferase 2 (MpLuc2) was established by Takenaka et al. [17]. (D) A single-sequence alignment (SSA) of ALuc30 using CLUSTALW 2.1 (NCBI). The alignment shows a characteristic three-storey structure. The arrow head shows putative dissection site in the sequence. Red boxes and gray shadows highlight consensus amino acids. The C-terminal end is designed like a bioluminescent capsule for carrying a protein of interest to the PM. (For interpretation of the references to color in this figure legend, the reader is referred to the web version of this article.)

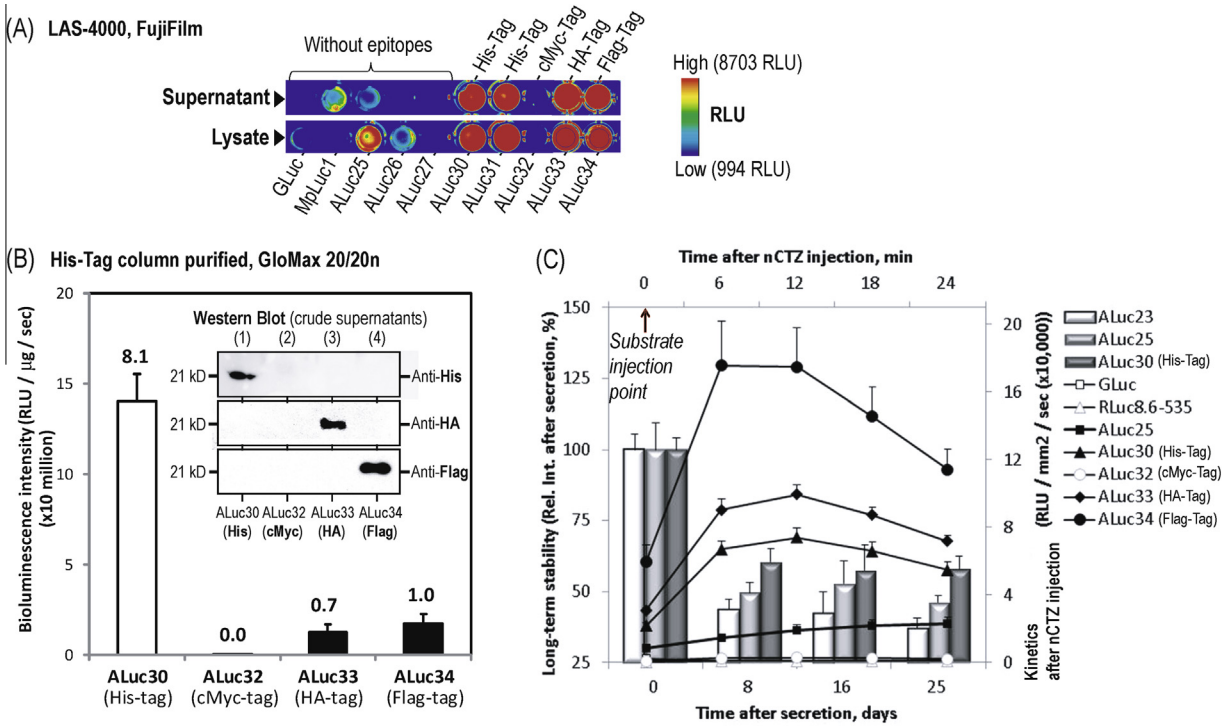

Fig. 2. Extracellular secretion of ALucs and the long-term stability of the optical intensities in the culture medium. (A) The optical activities of ALuc in cell lysate and extracellular compartment. In spite of the ER retention signal (KDEL), considerable amounts of ALucs are secreted into the extracellular compartment. (B) Relative optical intensities of ALucs 30–34 after His-tag column purification of the supernatants (n = 3). The absence of the ALuc32 band indicates the decomposition by misfolding in the host cells. Numbers on the bars indicate the fold intensity to ALuc34. The inset shows the results of Western blotting analysis. ALucs 30, 32, 33, and 34, secreted to supernatants, were electrophoresed in the lanes (1)–(4). (C) The long-term stability of ALuc activities after secretion (n = 4). Left and right axes indicate relative optical intensities for bar (long-term stability) and line (kinetics) graphs, respectively. The lower and upper axes show the time scale of the long-term stability test and the kinetics test, respectively.

25–34 using a lipofection reagent (TransIT-LT1, Mirus). As the internal references, the same COS-7 cells in the different wells of the microplate transiently transfected with the same amount of the plasmids encoding GLuc or MpLuc1 [8] were used. Sixteen hours after the transfection, the supernatants were carefully transferred to a new microplate, whereas the remaining cells were washed once with PBS and lysed with a lysis buffer (E291A, Promega). The luciferase activities of 10 μL of the supernatants or lysates on the microplates were determined with an image analyzer (LAS-4000, FujiFilm) after simultaneous injection of the specific substrate (native coelenterazine, nCTZ) in a luciferase assay kit (E2820, Promega).

The long-term optical stability of the secreted luciferases into the culture media was also determined every week until 25 days with the luciferase assay kit (solid bars, Fig. 2C). During the 25 days, the supernatants were sealed for preventing evaporation and stored in 4 °C. The short-term time course of the optical intensities of the 25-day-old luciferases was monitored for 25 min with the image analyzer after injection of nCTZ (marked lines, Fig. 2C). The obtained data were analyzed with a specific image-analyzing software for LAS-4000 (Multi Gauge ver3.1, FujiFilm).

The luminescence intensities were normalized by integration time and light-emitting area. The unit of absolute luminescence is subsequently expressed in relative luminescence unit per area–second of protein (RLU/mm^2/sec).

2.4. Western blot analysis of ALucs

Expression of the made ALucs was identified with Western blot (WB) analysis (Fig. 2B, inset), Coomassie brilliant blue (CBB) blotting (data not shown), and His-tag column purification (Fig. 2B). The detailed experimental methods were explained in Suppl. Method 1.

2.5. Substrate selectivity of ALucs

The substrate-specific bioluminescence of the made ALucs were examined in the presence of various coelenterazine analogs (Fig. 3). The COS-7 cells expressing one of ALucs 23–34 were prepared according to the same procedure as in Fig. 2A. As the internal references, COS-7 cells expressing GLuc or RLuc8.6-535 were used. Sixteen hours after the transfection, 10 μL of the lysates were carefully transferred to a fresh microplate, simultaneously mixed with 30 μL of each coelenterazine variant (CTZ *i*, CTZ *ip*, CTZ *cp*, CTZ *hcp*, CTZ *h*, CTZ *n*, CTZ *f*, CTZ *fcp*, CTZ *400A*) using a multichannel pipet, and placed in the image analyzer (LAS-4000). The relative optical intensities were immediately integrated for 5 s (Fig. 3A).

The luminescence intensities were normalized by integration time, light-emitting area, and the whole amounts of applied proteins determined by a Bradford reagent (Bio-Rad). The unit of absolute luminescence is subsequently expressed in relative luminescence unit per area–microgram–second (RLU/mm^2/μg/s).

The corresponding bioluminescence spectra were determined with a precision spectrophotometer (AB-1850, ATTO) (Fig. 3B), which can simultaneously acquire the full visible and near infrared ranges of emitted photons (i.e., 391–789 nm). For the study, the lysates were prepared according to the same procedure as in Fig. 2A. Immediately after mixing 5 μL of the lysates with the assay solution carrying CTZs *f*, *i*, or *ip*, the consequent bioluminescence spectra were determined with the spectrophotometer (ATTO) in an integration time of 10 s.

2.6. Prediction of the supersecondary structures of ALuc30 with a template-based modeling

The molecular structure of ALuc30 was predicted by a template-based modeling of the amino acid sequence (Fig. 4). The detailed

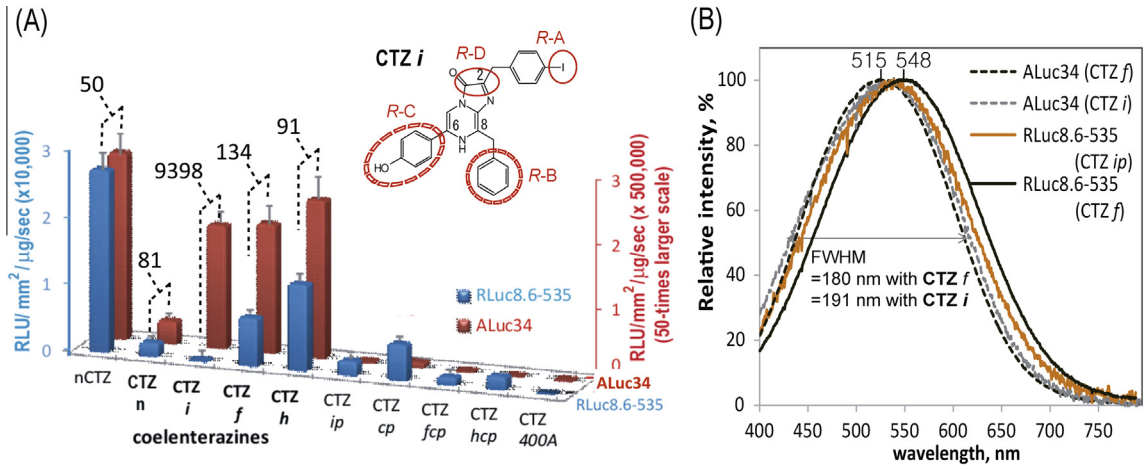

Fig. 3. Substrate-specific optical activities of ALucs. (A) Comparison of absolute optical intensities of RLuc8.6-535 (blue) and ALuc34 (red) ($n = 4$). The left and right axes indicate optical intensities of RLuc8.6-535 and ALuc34, respectively, where the axis scale for ALuc34 is 50-times larger than that for RLuc8.6-535 (i.e., ALuc34 emits 50-times stronger absolute intensities than RLuc8.6-535). The numbers on the bars indicate relative optical intensities of ALuc34, when compared with RLuc8.6-535, in response to the same substrates. The inset shows the chemical structure of CTZ *i*, which is highly specific to ALucs. The red circles highlight key side chains that may determine the substrate specifcity to ALucs. (B) The bioluminescence spectra of RLuc8.6-535 and ALuc34 normalized in percentage. FWHM means the full width at half maximal intensity in wavelength. The spectra were measured in triplicate.

procedure of the present template-based modeling (TBM) approach was previously demonstrated [10].

In brief, we reviewed the known crystallographic information of existing marine luciferases available from public databases. When we chose CBP for the structural template of ALucs, we considered that (i) ALucs share a similar light-emitting mechanism with RLuc (e.g., no cofactors), rather than photoproteins including Ca^{2+}-sensitive aequorin, (ii) ALucs share the highest sequence homology with the coelenterazine-binding protein (CBP) derived from *R. muelleri* (PDB id: 2hps and 2hq8) (16.7%) among structure-available luciferases in public databases, and (iii) the other molecular features including the substrate and molecular weight are close to CBP. The main chain character for each amino acid peptide unit in CBP was assigned to three conformational patterns, α-helical (*h*), β-sheet (*s*), and the other (*o*) types in the view of the supersecondary structure. The sequence of CBP was aligned with that of ALuc30 in view of the above-assigned supersecondary structure. In the alignment, every consensus amino acids in CBP were first substituted with the ones of ALuc30 using MolFeat v4.5 (FiatLUX). Regarding mismatched, access, or missed amino

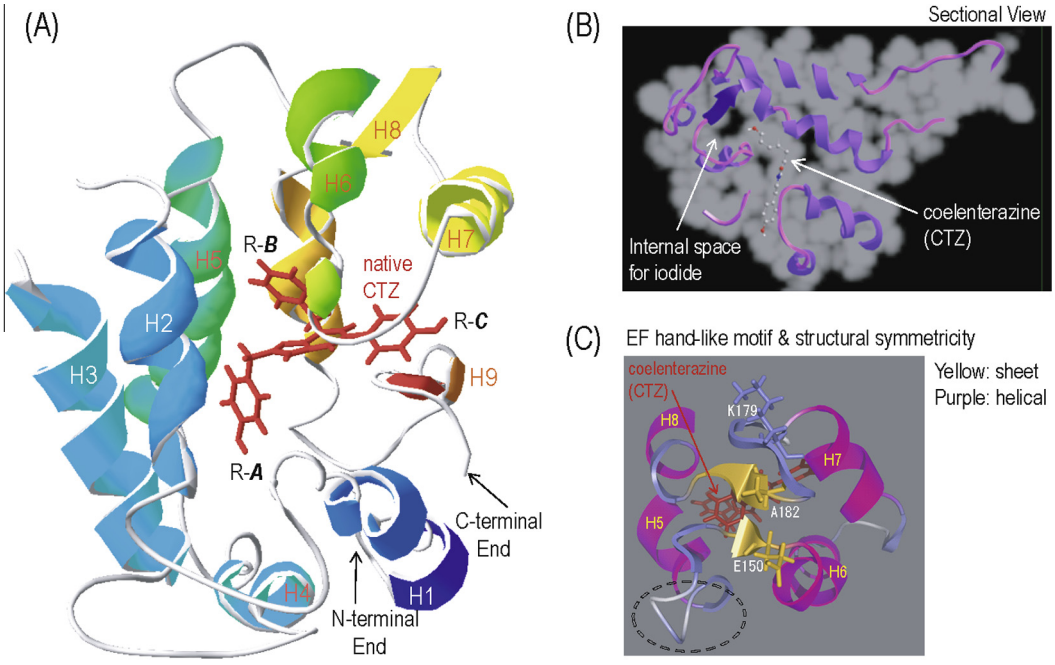

Fig. 4. Predicted supersecondary structure of ALuc30 with respect to the X-ray crystallographic information of the coelenterazine-binding protein (CBP) of *R. muelleri* (PDB: 2hps and 2hq8). (A) A color view of the supersecondary structure of ALuc30. The chemical structure in red shows native coelenterazine. The helices were numbered H1-H9 in a descending order from the N-terminal. The detailed information on the supersecondary structure is provided in Suppl. Tables. (B) A sectional view of the supersecondary structure of ALuc30. The sectional view shows an internal space for accommodating the iodide of CTZ *i*. (C) The symmetric structure of EF hand-like motifs and β-sheets. The dotted circle shows a part of the EF hand-like motif. The central β-sheets are marked in yellow. The red bars show the substrate, while the other bars exhibit side chains of E150, K179, and A182. (For interpretation of the references to color in this figure legend, the reader is referred to the web version of this article.)

acids in the alignment, we carefully tried a further molecular modeling with specific softwares, HyperProtein v1.0 (HuLinks) and Chem3D Ultra v8.0 (Cambridge soft), so that the aligned sequences reach a close consensus on the supersecondary structures. Finally, the molecular structure of ALuc30 was optimized by a molecular mechanics (MM) calculation based on a Polak–Ribiere algorithm.

3. Results and discussion

Although luciferases are an excellent optical readout, native luciferases themselves are less functional for bioassays. It is because it does not carry any on–off switches for bioassays and epitope or purification tags for lab-on-a-chip devices. Instead, many luciferases have been smartly engineered to create novel optical indicators, which are categorized into basic, inducible, and activatable groups according to the working mechanisms [11]. Many of the activatable indicators utilize a basic strategy of temporal dissection and reconstitution of luciferase fragments [1].

Conventional tagging schemes for proteins are invalid for copepod luciferases, because the N-terminal end is naturally removed in the ER during the secretion process, while the C-terminal end is a part of the active site and thus tagging to it invades the optical intensities (Fig. 4A). To address the limited functionality, we designed ALucs 30–34, which carry epitopes (Fig. 1A and B). The epitopes are situated at the downstream of the secretion peptide (SP), in contrast to the conventional method of tagging the epitopes at the N- or C-terminal ends. Thus, the epitope after secretion is naturally exposed to the extracellular circumstance for purification and immunoassays.

The relative optical intensities of ALucs 30–34 were determined in comparison with those of GLuc and MpLuc1 (Fig. 2A), or RLuc8.6-535 (Fig. 3). The optical intensities of ALucs 30, 33, and 34 in supernatants were 49, 68, 24-times stronger than that of GLuc, respectively. The similar feature was observed in the comparison among the lysates. Further, considerable amounts of the ALucs 30, 33, and 34 were found to be leaked from the intracellular compartments, although the ALucs carry an ER retention signal (KDEL) (Fig. 2A). The poorest optical intensities of ALuc32 suggest that the *c*-Myc sequence in ALuc32 may hamper a proper folding of ALuc32 or exerts dysfunction of any key amino acids for the activity.

It is interesting to discuss the secretion efficiency between ALuc25 and ALuc30 series luciferases (Fig. 2A). The initial 30 AAs including the putative secretion peptide (SP) (1–20 AAs) of the luciferases [2,12] are supposed to determine the secretion efficiency. A drastic hydrophilicity conversion is found before and after the dissection site of the SP at the AA numbers 18–20. The secretion efficiency variance between ALuc25 and ALuc30 series luciferases is explained with the distinctive initial SP sequences. ALucs 30, 32, and 34 share the same SP sequence (1–20 AAs) and secretion efficiency with each other. This overall comparison suggests that the secretion efficiency of ALucs is dominated by the former SP sequence (1–20 AAs) rather than the rear sequence (21–30 AAs; various sites) at the initial N-terminal region.

Secretion of the ALucs 30–34 was estimated with WB analysis of the supernatants (Fig. 2B, inset). Anti-His, anti-HA, and anti-Flag antibodies recognized specific bands of ALucs 30–34 at 21 kD, of which electrophoretic mobility was consistent with the predicted size of the luciferases after secretion.

To further ensure that ALuc30 carrying His-tag is properly secreted into the extracellular compartment, ALucs 30–34 in the supernatants were simultaneously purified with a His-tag affinity column (GE Healthcare) (Fig. 2B) and found that His-tag-carrying ALuc30 exerts approximately eight-times stronger bioluminescence than ALuc34, where the net amount of the expressed ALuc30 is almost equivalent with ALucs 33 and 34 according to the CBB blotting result. The relatively weak bioluminescence suggests that a small amount of ALucs 33 and 34 is retained in the column, although they contain no His-tag. The absence of bioluminescence and a western blot band of ALuc32 suggests that ALuc32 failed to properly fold up in the host cells.

The long-term optical intensity of epitope-bearing ALucs was evaluated with the ALucs leaked into supernatants (Fig. 2C, bars, left axis). The optical intensities were estimated by time for 25 days. The relative luciferase activities of ALucs 23, 25, and 30 were gradually decreased by time after secretion. ALuc30 maintained approximately 58 ± 5% of the original activities even 25 days after secretion, whereas ALuc23 kept only 37 ± 4% in the same condition.

Time course of the optical intensities of 25-day-old ALuc supernatants was also monitored during 25 min after simultaneous injection of nCTZ to the supernatant samples (Fig. 2C, marked lines, right axis). Interestingly, the optical intensities by ALucs 30, 33, and 34 were gradually increased by time and reached a plateau at around 10–12 min after nCTZ injection. This growing optical profile is characteristic from other existing CTZ-consuming marine luciferases including copepod luciferases, which generally emit flashing bioluminescence. This time-intensity profile may be explained with the large amount of serum albumins in the culture medium, blocking ALuc activities. The ALucs were stocked in a 4 °C refrigerator, where they may be in the form of aggregaton for 25 days. The aggregated ALucs should not exert full enzymtic activities immediately after the substrate injection.

The phylogenetic analysis and sequential identities of the made luciferases is distinctive from any existing luciferases (Fig. 1C and Suppl. Fig. 1). This feature inspired us to further investigate (i) the probability of an optimal substrate for ALucs in light of the chemical structures of coelenterazine derivatives (Fig. 3), and (ii) the molecular structural characteristics of ALucs.

The relative optical intensities were decreased in the order of CTZs *h*, *f*, *i*, and *n*. Interestingly, this order is the same as the size of the benzyl residue at the position 2 (*R*-**A**): i.e., CTZ *h* does not have any functional group in the benzyl backbone, whereas CTZ *n* carries the largest functional group (naphthalene) at the same position (Suppl. Fig. 2). A dramatic optical contrast was found with a coelenterazine variant, CTZ *i*, where ALuc34 surprisingly exerts ca. 9400-times stronger bioluminescence than RLuc8.6-535 in the presence of CTZ *i* (Fig. 3A). This drastic specificity was relieved with CTZs *f*, *h*, *n*. This size-driven feature strongly suggests that the drastic substrate selectivity of ALuc34 to CTZ *i* is derived by the size effect of the benzyl group at position 2 to the substrate-binding pocket of ALuc34. Iodide is a rarely occurring atom in natural proteins and fills a larger space in the binding pocket of ALucs than other atoms. This view on size effect is also supported by a previous study on newly synthesized coelenterazine analogs for RLucs [13].

The bioluminescence spectra were determined according to the substrates (Fig. 3B). The maximal optical intensities (λ_{max}) of ALuc34 with CTZs *f* and *i* are ca. 515 and 526 nm, respectively, while λ_{max} values of RLuc8.6-535 with CTZs *ip* and *f* are ca. 537 and 548 nm, respectively. The results indicate that RLuc8.6-535 exhibits generally more red-shifted bioluminescence than ALuc34 with the same substrate. The gap between the λ_{max} values of ALuc34 and RLuc8.6-535 is ca. 33 nm in the presence of CTZ *f*. The full width at half maximum (FWHM) values of ALuc34 with CTZs *f* and *i* were 180 and 191 nm, respectively.

Estimation of the spatial position of all the amino acids in ALucs is a valuable approach for a precise investigation of the optical properties of ALucs. Since template-based modeling (TBM) is the only reliable method for high-resolution structure prediction [14,15], we predicted the supersecondary structure of ALuc30 with respect to the X-ray crystallographic information of CBP (PDB:

2hps and 2hq8). The consequently proposed molecular structure of ALuc30 consists of nine α-helical structures and a cave for accommodating the substrate (Fig. 4). The analysis on the supersecondary structure revealed EF hand-like motifs between Helices 5 and 6, and Helices 7 and 8 (from V140 to A152 and from G174 to K186; Fig. 4C). The helices carrying the motifs show a symmetric repeat, in which the center of the symmetry is found between two antiparallel sheets**.** Interestingly, the deepest end of the cave provides a large hole for iodide of CTZ *i*, exerting the excellent substrate specificity to CTZ *i*. In contrast to the promising result in this study, precedent literatures have reported that CTZ *i* is one of the poorest substrates for the existing marine luciferases and photoproteins [16]. This drastic contrast is explainable by a unique size selection effect of the ALuc pocket to the residues of CTZ, different from the existing marine luciferases.

Acknowledgments

This work was supported by the Japan Society for the Promotion of Science (JSPS) Grant-in-Aid for Scientific Resech (B) (Grant number: 26288088).

Appendix A. Supplementary data

Supplementary data associated with this article can be found, in the online version, at http://dx.doi.org/10.1016/j.bbrc.2014.04.128.

References

[1] T. Ozawa, H. Yoshimura, S.B. Kim, Advances in fluorescence and bioluminescence imaging, Anal. Chem. 85 (2013) 590–609.
[2] Y. Takenaka, A. Yamaguchi, N. Tsuruoka, M. Torimura, T. Gojobori, Y. Shigeri, Evolution of bioluminescence in marine planktonic copepods, Mol. Biol. Evol. 29 (2012) 1669–1681.
[3] S.B. Kim, Labor-effective manipulation of marine and beetle luciferases for bioassays, Protein Eng. Des. Sel. 25 (2012) 261–269.
[4] A.M. Loening, T.D. Fenn, A.M. Wu, S.S. Gambhir, Consensus guided mutagenesis of *Renilla luciferase* yields enhanced stability and light output, Protein Eng. Des. Sel. 19 (2006) 391–400.
[5] W.P. Russ, D.M. Lowery, P. Mishra, M.B. Yaffe, R. Ranganathan, Natural-like function in artificial WW domains, Nature 437 (2005) 579–583.
[6] S.B. Kim, M. Torimura, H. Tao, Creation of artificial luciferases for bioassays, Bioconjug. Chem. 24 (2013) 2067–2075.
[7] S. Inouye, Y. Sahara, Identification of two catalytic domains in a luciferase secreted by the copepod *Gaussia princeps*, Biochem. Biophys. Res. Commun. 365 (2008) 96–101.
[8] S.B. Kim, H. Suzuki, M. Sato, H. Tao, Superluminescent variants of marine luciferases, Anal. Chem. 83 (2011) 8732–8740.
[9] S.B. Kim, Y. Ito, M. Torimura, Bioluminescent capsules for live-cell imaging, Bioconjug. Chem. 23 (2012) 2221–2228.
[10] H. Izumi, A. Wakisaka, L.A. Nafie, R.K. Dukor, Data Mining of supersecondary structure homology between light chains of immunogloblins and MHC molecules: absence of the common conformational fragment in the human IgM rheumatoid factor, J. Chem. Inf. Model. 53 (2013) 584–591.
[11] G. Niu, X.Y. Chen, Molecular imaging with activatable reporter systems, Theranostics 2 (2012) 413–423.
[12] T.N. Petersen, S. Brunak, G. von Heijne, H. Nielsen, SignalP4.0: discriminating signal peptides from transmembrane regions, Nat. Methods 8 (2011) 785–786.
[13] G. Giuliani, P. Molinari, G. Ferretti, A. Cappelli, M. Anzini, S. Vomero, T. Costa, New red-shifted coelenterazine analogues with an extended electronic conjugation, Tetrahedron Lett. 53 (2012) 5114–5118.
[14] A. Roy, Y. Zhang, Protein Structure Prediction, eLS, John Wiley & Sons Ltd, U.S.A., 2001.
[15] A. Roy, J.Y. Yang, Y. Zhang, COFACTOR: an accurate comparative algorithm for structure-based protein function annotation, Nucleic Acids Res. 40 (2012) W471–W477.
[16] O. Shimomura, B. Musicki, Y. Kishi, Semi-synthetic aequorins with improved sensitivity to Ca^{2+} ions, Biochem. J. 261 (1989) 913–920.
[17] Y. Takenaka, H. Masuda, A. Yamaguchi, S. Nishikawa, Y. Shigeri, Y. Yoshida, H. Mizuno, Two forms of secreted and thermostable luciferases from the marine copepod crustacean, *Metridia pacifica*, Gene 425 (2008) 28–35.